ELECTRODE-CONFINED CATALYST SYSTEMS FOR USE IN OPTICAL-TO-CHEMICAL ENERGY CONVERSION*

KAREN A. DAUBE, D. JED HARRISON, THOMAS E. MALLOUK, ANTONIO J. RICCO, SHUCHI CHAO and MARK S. WRIGHTON

Department of Chemistry, Massachusetts Institute of Technology, Cambridge, MA 02139 (U.S.A.)

WILLIAM A. HENDRICKSON and ARNOLD J. DRUBE

Central Research Laboratory, 3M Company, St. Paul, MN 55144 (U.S.A.)

Summary

Catalysis of multiple-electron transfer fuel-forming redox reactions at illuminated semiconductor–liquid electrolyte interfaces is important in achieving efficient optical energy conversion. The characterization of redox polymer–noble metal combinations as catalysts for the reduction of H_2O and aqueous CO_2 is described in this article. Emphasis is on the demonstration of rational synthetic methods applied to interfaces and the correlation of surface structure and function.

1. Introduction

Catalysis of light-driven redox processes at semiconductor–liquid electrolyte interfaces has yielded significant advances in the efficiency for the conversion of solar energy to chemical energy. Particular success has been achieved for the catalysis of photoelectrochemical H_2 evolution at p-type semiconductor photocathodes where gross decomposition of the semiconductor is usually not a problem [1 - 5]. However, the catalysis of photoanode processes is also important. The I_3^-–I^- mediated oxidation of SO_2 [6] and catalyzed Cl_2 generation [7] at n-type metal dichalcogenide photoanodes represent systems where high efficiency depends on rate improvement of the desired oxidation process. Since many of the fuel-forming reactions of interest in solar conversion involve multiple-electron transfer processes and these are generally kinetically sluggish at electrodes, better and less costly electron transfer catalysts will probably be necessary to develop practical solar production of useful fuel.

*Paper presented at the Fifth International Conference on Photochemical Conversion and Storage of Solar Energy, Osaka, Japan, August 26 - 31, 1984.

0047-2670/85/$3.30

We have been especially interested in the catalysis of reduction processes at electrodes derivatized with the viologen reagent I [4, 5]:

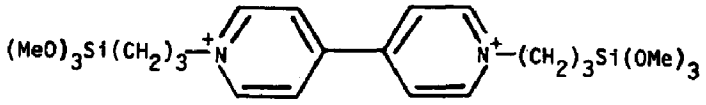

I

More recently, the cobalticenium-based reagent II

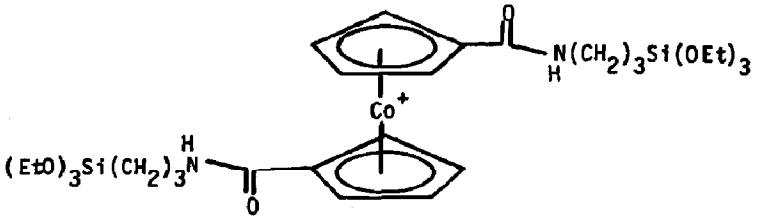

II

has been synthesized and shown to be useful as an electrode derivatizing reagent [8]. In this article we wish to summarize some of our recent results on the characterization of electrode catalysts derived from the combination of I and noble metals such as palladium, platinum and rhodium [9, 10]. Further, we summarize findings relating to a new surface modification procedure for p-InP to catalyze photoelectrochemical H_2 generation using reagent II and deposited rhodium [11] and describe a catalyst system for the electrochemical and photoelectrochemical reduction of aqueous CO_3H^- [12].

The work described herein concerns the study of electrode/catalyst assemblies like those illustrated in Figs. 1(a) and 1(b). In the assembly shown in Fig. 1(a) the noble metal (palladium, platinum or rhodium) is confined to

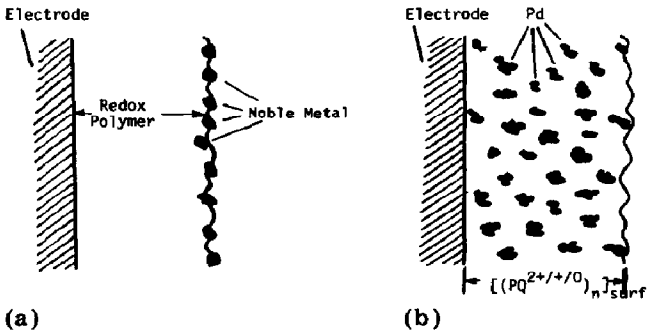

(a) (b)

Fig. 1. (a) Electrode/catalyst assembly for H_2 evolution and (b) electrode/catalyst assembly for reduction of aqueous CO_3H^-.

the outermost portions of the redox polymer $[(PQ^{2+/+/0})_n]_{surf}$ from I or the redox polymer $[(CoL_2^{+/0})_n]_{surf}$ from II by electrochemically depositing the metal onto the one-electron reduced polymer [4, 8 - 10]. The uniformly dispersed palladium in the assembly shown in Fig. 1(b) is achieved by exchanging the charge-compensating anions of $[(PQ^{2+}\cdot 2Br^-)_n]_{surf}$ with $PdCl_4^{2-}$ followed by electrochemical reduction of the bound $PdCl_4^{2-}$ to palladium metal [4].

2. Results and discussion

2.1. Synthesis and Auger spectroscopic characterization of a structured catalyst assembly

The general methodology for the preparation of the structured assembly represented by Fig. 1(a) is to derivatize an electrode with I or II to give a uniform pinhole-free redox polymer film. It would appear that for I coverages of about 10^{-8} mol cm^{-2} are sufficient to cover the electrode surfaces completely [4]. The noble metal can then be deposited from an aqueous solution of $PdCl_4^{2-}$, for example, by holding the electrode at a potential where the surface polymer from I or II is in the reduced state [4, 8 - 10]. The evidence that an assembly as shown in Fig. 1(a) results comes from Auger spectra recorded while sputtering the surface with Ar^+ ions. Figure 2 shows the Auger spectrum of the outer surface of an electrode/$[(PQ^{2+}\cdot 2Cl^-)_n]$/Pd_{surf} system and the so-called depth profile analysis [13]. The crucial point is that palladium is confined to the outermost portions of the polymer and does not directly contact the underlying electronic conductor. Thus, the only mechanism for equilibration of the electrode with palladium is via the intervening polymer. Similarly structured interfaces can be prepared using other metals (platinum or rhodium) and polymers derived from II. Figure 3 illustrates the Auger depth profile analysis of a p-Si/$[(CoL_2^+\cdot X^-)_n]$/Rh_{surf} photocathode/catalyst assembly [8].

Transmission electron microscopy [13, 14] has been used to examine the noble metal deposited onto polymers derived from I. (Transmission electron micrographs were obtained on a Philips model EM 200 microscope at the 3M Central Research Laboratories. The methodology employed is as described in ref. 14. Approximately 20 Å of carbon was vapor deposited onto the sample surface to form a carbon envelope around the metal microislands. The carbon film containing the palladium or platinum was removed from the $[(PQ^{2+})_n]_{surf}$ film and/or the tungsten substrate by immersion of the sample in 20% HF in such a way that the film floated on the solution surface. The carbon film was then lifted from the solution surface on a 200 mesh copper transmission electron microscope grid. Micrographs were made by through-focusing until any microislands were imaged.) Figure 4 illustrates the difference between palladium and platinum deposited onto $[(PQ^{2+/+})_n]_{surf}$. The palladium is shown to be more uniformly deposited than the platinum, but in both cases the particle size of the metal is small (less than 200 Å).

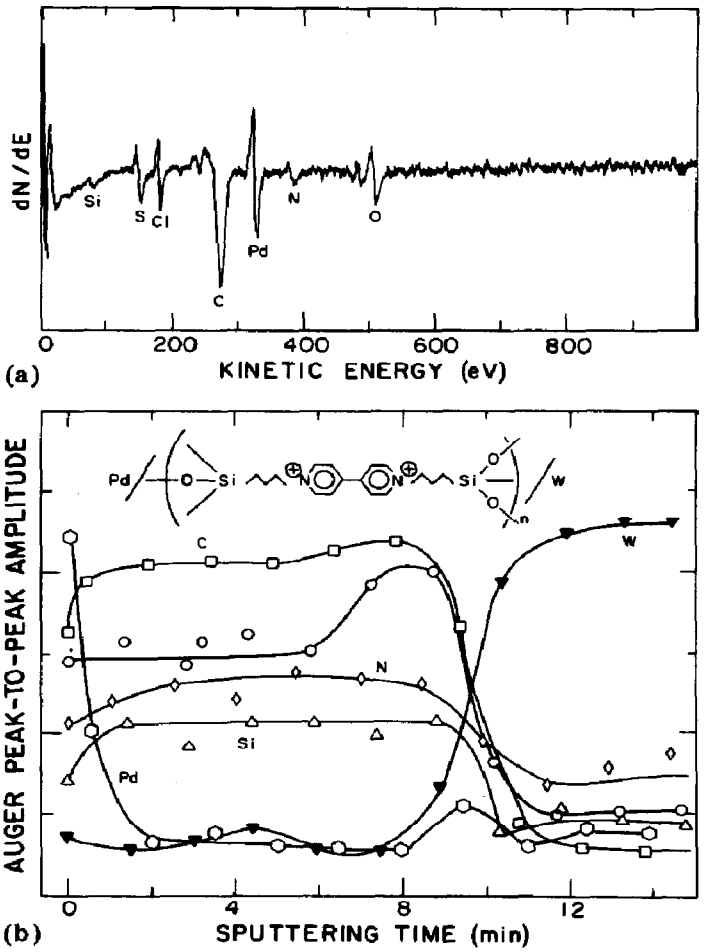

Fig. 2. (a) Auger electron spectrum of palladium on $[(PQ^{2+}\cdot 2Cl^{-})_n]_{surf}$ on a tungsten substrate with a 5 keV, 2 μm, 150 nA electron beam as the excitation source. (b) Auger depth profile of $Pd/[(PQ^{2+}\cdot 2Cl^{-})_n]_{surf}/W$ recorded while sputtering with 2 keV Ar^{+} ions at an ion current density of about 25 $\mu A\ cm^{-2}$. Depth-dependent signals for palladium (×1), carbon (×4/3), nitrogen (×4), oxygen (×2), silicon (×7/3) and tungsten (×1) are shown. The coverage of palladium was about 2×10^{-8} mol cm^{-2} and that of $[(PQ^{2+}\cdot 2Cl^{-})_n]_{surf}$ was about 4×10^{-8} mol cm^{-2}.

At the coverages shown there is obviously a non-continuous film of metal. In general, cyclic voltammetry (sweep rate, 50 mV s^{-1}) in an aqueous electrolyte solution of electrodes derivatized with polymers from I is unaffected by the deposition of metal even for amounts exceeding 10^{-7} mol cm^{-2}.

The electrode/catalyst assembly represented by Fig. 1(b) can be prepared by first derivatizing the electrode with I and then exchanging counter-ions with $PdCl_4^{2-}$ and (photo)electrochemical reduction of the palladium(II) to palladium(0) [4]. For such an assembly the Auger depth profile analysis shows palladium(0) throughout the polymer [4].

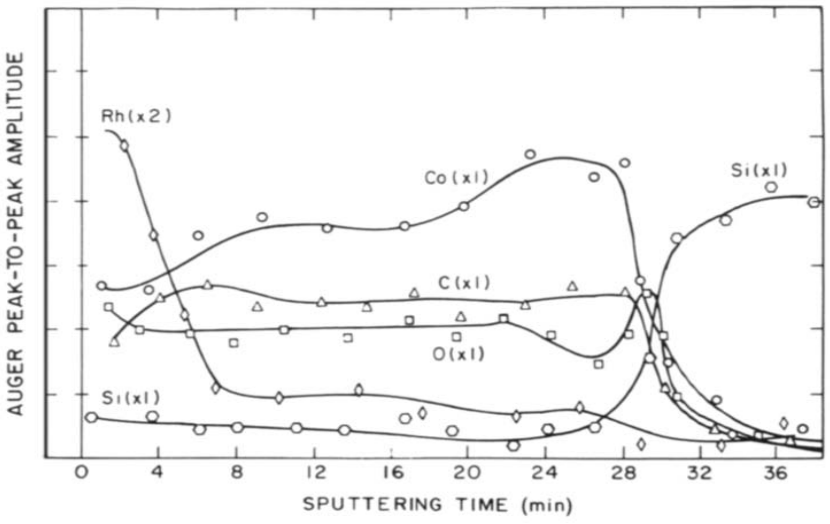

Fig. 3. Auger depth profile analysis of a p-Si/$[(CoL_2^{+}\cdot Cl^{-})_n]$/$Rh_{surf}$ interface (coverage of the polymer, 6×10^{-8} mol cm^{-2}; coverage of the rhodium, 2.5×10^{-8} mol cm^{-2}).

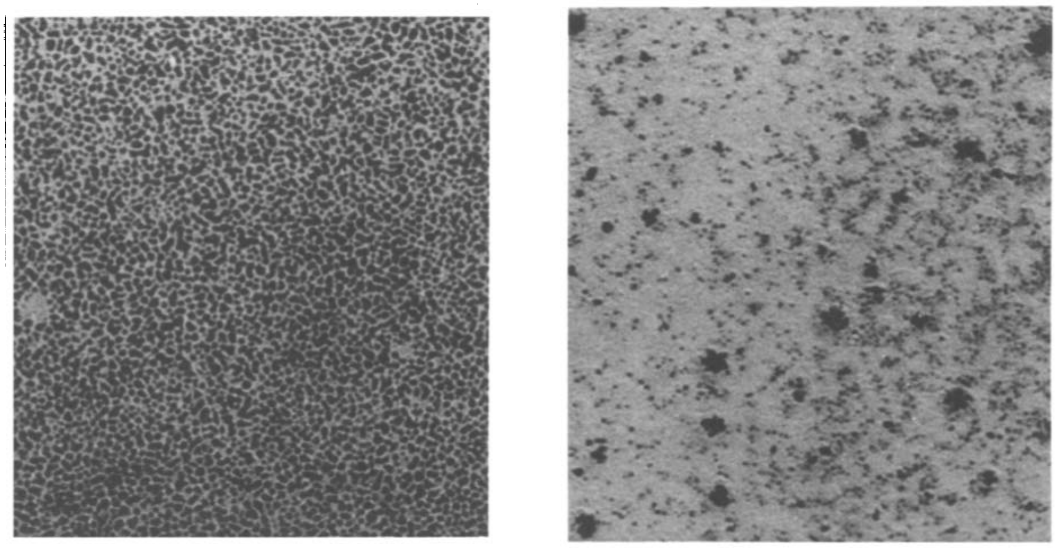

(a) (b)

Fig. 4. Transmission electron micrographs of 2×10^{-8} mol cm^{-2} (a) of palladium and (b) of platinum electrodeposited onto a $[(PQ^{2+})_n]_{surf}$ film at −0.60 V measured with respect to a standard calomel electrode (SCE) from a solution of 15 μM MCl_4^{2-} (M = Pd, Pt) and 1 M KCl (see for example refs. 13 and 14). The dark spots are the metal particles.

2.2. Catalytic activity of palladium, platinum and rhodium deposited onto redox polymers

For the interfaces represented by Fig. 1(a) it is possible to assess quantitatively the catalytic activity of the deposited noble metal for the H_2 evolu-

tion reaction. By confining the catalyst to the outermost surface of the polymer, the catalytic activity of the system is restricted to that region. Accordingly, the situation fits one of the limiting cases treated by Saveant and coworkers [15], allowing the following relationship

$$\frac{1}{i_{obs}} = \frac{1}{i_L} + \frac{1}{i_E} + \frac{1}{i_k} + \left(\frac{1}{K} - 1\right)\frac{i_{obs}}{i_E i_L} \tag{1}$$

between the observed current i_{obs} at a rotating disk electrode, the polymer-limited current i_E, the (Levich) mass-transport-limited current i_L [16] and the kinetic current i_k. In eqn. (1), K is the equilibrium constant for the reaction involving the redox polymer and the substrate. Since the formal potential $E^{\circ\prime}$ of $[(PQ^{2+/+})_n]_{surf}$ is independent of pH [4, 5] and $E^{\circ\prime}(H_2O/H_2)$ is pH dependent, the value of K can be adjusted by varying the pH for a fixed redox potential. When K is large, eqn. (1) simplifies to

$$\frac{1}{i_{obs}} = \frac{1}{i_L} + \frac{1}{i_E} + \frac{1}{i_k} - \frac{i_{obs}}{i_E i_L} \tag{2}$$

The catalyst assembly in Fig. 1(a) may give an H_2 evolution rate that is limited by (i) the charge transport properties of the redox polymer (i_E limited), (ii) the catalytic activity of the metal (i_k limited), (iii) the flux of reducible material (i_L limited) or (iv) a combination of two or more of these. Here we are concerned with the value of i_k. The metal used as catalyst and its coverage should cause variations in i_k [17]. Figure 5 illustrates the situation, showing the polymer charge transport i_E and the catalyst current i_k.

For $[(PQ^{2+/+})_n]_{surf}$ the value of i_E, the maximum current that can be passed through the polymer film, can be determined by measuring the current for the mediated reduction of $Ru(NH_3)_6^{3+}$ at a derivatized rotated disk [18, 19]:

$$[(PQ^{2+})_n]_{surf} \xrightarrow{ne^-} [(PQ^{+})_n]_{surf} \tag{3}$$

$$[(PQ^{+})_n]_{surf} + Ru(NH_3)_6^{3+} \xrightarrow{k_{et}} [(PQ^{2+})_n]_{surf} + nRu(NH_3)_6^{2+} \tag{4}$$

The value of k_{et} is so large [18, 19] (giving a very large value of i_k) that it is very easy to find conditions where $i_{obs} \approx i_E$. Equation (2) applies in this

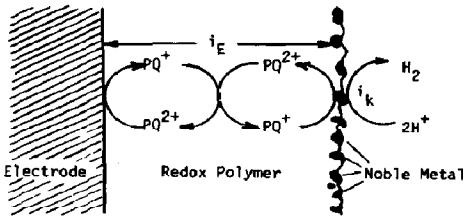

Fig. 5. Polymer/catalyst system for H_2 evolution.

case since the $Ru(NH_3)_6^{3+}$ does not significantly penetrate the $[(PQ^{2+/+})_n]_{surf}$ polymer and K exceeds 10^4 [19]. Importantly, the same value of i_E is found for disk electrodes only derivatized with I [19] and for electrodes derivatized with I followed by deposition of a noble metal [9, 10]. For coverages of about 5×10^{-8} mol cm^{-2} of I, i_E is in the vicinity of 10 - 15 mA cm^{-2} in 1.0 M KCl of pH 2.8 made acidic with HCl [9, 10]. The value of i_E is inversely proportional to the thickness of the polymer and sufficiently thin, but pinhole-free, films of $[(PQ^{2+/+})_n]_{surf}$ give i_E values that significantly exceed 30 mA cm^{-2}.

At a sufficiently large rotation velocity for a rotating disk electrode or where mass transport does not limit the value of i_{obs}, the observed current for a mediated reduction process at the outer surface of the catalyst assembly would be given by [9, 10]

$$\frac{1}{i_{obs}} = \frac{1}{i_E} + \frac{1}{i_k} \tag{5}$$

In order to achieve high efficiency solar devices it is important that the only current-limiting factor be light intensity. Under air mass 1 illumination the optimum solar devices would give a value of i_{obs} of the order of 25 mA cm^{-2}. Accordingly, it is important to find redox polymers with i_E values that significantly exceed 25 mA cm^{-2} as well as catalysts that give values of i_k well in excess of 25 mA cm^{-2}. There is the additional objective of delivering more than 25 mA cm^{-2} with the least amount of driving force, since the driving force diminishes the photovoltage. Finally, for photoelectrode catalysts there is the requirement that the catalyst assembly be optically transparent and, if absorbing, photoinert. There is intense visible absorption for $[(PQ^{+})_n]_{surf}$ (λ_{max} = 550 nm, $\epsilon \approx 10^4$ M^{-1} cm^{-1}) [20], but at coverages where i_E would significantly exceed 25 mA cm^{-2} (less than 1×10^{-8} mol cm^{-2}) the extinction of the visible light would be less than about 10% even when all the electrode-bound polymer is in the $[(PQ^{+})_n]_{surf}$ state. The optical properties of $[(CoL_2^{0})_n]_{surf}$ are even more favorable in this regard: λ_{max} = 460 nm; $\epsilon \approx 10^3$ M^{-1} cm^{-1} [8]. However, the deposited metals do absorb incident light and it is therefore important to minimize the amount of metal deposited. Naturally, minimization of the amount of noble metal is also impelled by the high cost of such materials. Indeed, there is justifiable effort to find catalysts for fuel-forming reactions that do not employ expensive noble metals. The naturally occurring enzyme hydrogenase, having no noble metals, will catalyze H_2 evolution at a rate of about 10^3 s^{-1} per site (see for example ref. 21). This rate is sufficiently high to give an i_k value of 10 mA cm^{-2} if the coverage of the catalyst is 10^{-10} mol cm^{-2}. The point is that effective catalysts for fuel-forming reactions exist; it is important to develop protocols for evaluating them in quantitative terms.

One set of rotating disk electrode measurements has been carried out for $[(PQ^{+})_n]/Pd_{surf}$ disk surfaces and the conclusion drawn was that eqn. (2) applies for 1.0 M KCl solutions of pH 2.8 for an electrode held at −0.78 V (SCE) where the polymer is in the one-electron reduced state [9, 10]. For

palladium coverages of more than 1×10^{-7} mol cm^{-2}, i_k values of more than 30 mA cm^{-2} for H_2 evolution can be obtained. Thus, by using sufficiently thin films of $[(PQ^{2+/+})_n]_{surf}$ coated with palladium it should be possible to achieve a solar-limited current for H_2 evolution.

By using *buffered* solutions of pH 2.8, the available proton flux at a rotating disk electrode can be much higher than that in the unbuffered 1.0 M KCl solutions of pH 2.8 used to characterize [9] the palladium on $[(PQ^{+})_n]_{surf}$. Experiments have been carried out in a solution of 0.2 M $ClCH_2COOH$ and 1 M KCl, adjusted to pH 2.8 with aqueous NH_3, to measure the metal dependence of i_k when eqn. (5) should apply. A rotating naked platinum disk electrode (held at −0.78 V (SCE)) gives a linear plot for i_{obs} *versus* $\omega^{1/2}$ up to $\omega^{1/2} = 16$ where i_{obs} is about 80 mA cm^{-2} for H_2 evolution. For coverages of $[(PQ^{2+})_n]_{surf}$ of about $(4 - 5) \times 10^{-8}$ mol cm^{-2} the value of i_E was found to be 11 - 16 mA cm^{-2} from rotating disk experiments for the reduction of 50 mM $Ru(NH_3)_6^{3+}$ in 1 M KCl of pH 2.8 ($ClCH_2COOH$ buffered). For such solutions the reduction current for the mediated reduction of $Ru(NH_3)_6^{3+}$ is essentially independent of the rotation velocity, since i_{obs} is controlled by i_E. Figure 6 shows the value of i_{obs} for H_2 evolution at $\omega^{1/2} = 16$ and an electrode potential of −0.78 V (SCE) for rotating disk electrodes derivatized with

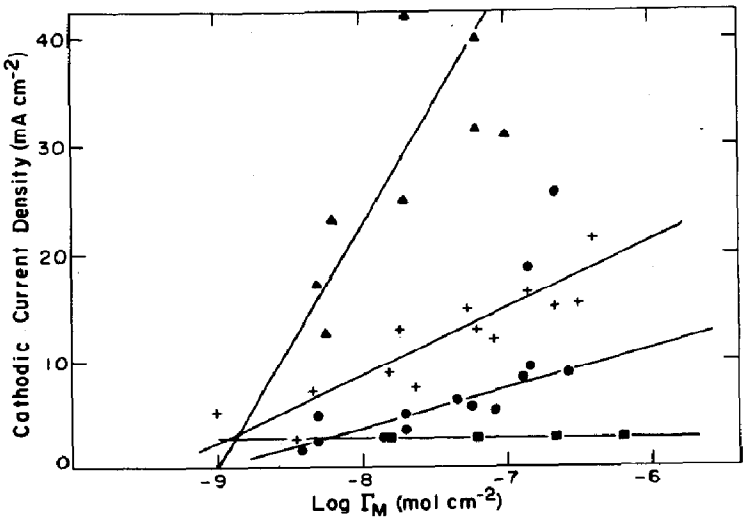

Fig. 6. Plot of current density for H_2 evolution at indium tin oxide (ITO)/$[(PQ^{2+})_n]$/M_{surf} electrodes as a function of Γ_M ($\omega^{1/2} = 16$; electrode potential (potentiostatted), −0.78 V (SCE); solution, 0.2 M $ClCH_2COOH$ and 1 M KCl; pH 2.8): ▲, rhodium; +, platinum; ●, palladium; ■, silver. $\Gamma_{PQ^{2+}}$ was between 4×10^{-8} and 5×10^{-8} mol cm^{-2} and i_E varied from 11 to 16 mA cm^{-2}. (The deposition of silver, rhodium, palladium and platinum was effected by holding the electrode at a potential where the $[(PQ^{+})_n]_{surf}$ is present in 0.5 M $NaNO_3$, 1.0 M Na_2SO_4, 1.0 M KCl and 0.5 M $NaClO_4$ respectively, followed by the addition of $AgNO_3$, $Rh_2(SO_4)_3$, K_2PdCl_4 and *cis*-$Pt(NH_3)_2Cl_2$ respectively to bring the metal ion concentration to 20 - 50 μM. Plating was monitored by measuring the charge passed associated with the reduction of the metal ion.)

$(4 - 5) \times 10^{-8}$ mol cm^{-2} of $[(PQ^{2+})_n]_{surf}$ and various metals (silver, rhodium, palladium and platinum) at different coverages.

The data in Fig. 6 show that there is a strong dependence of i_{obs} on the deposited metal and its coverage. Clearly, silver is the least effective catalyst. This finding is consistent with the knowledge that silver has a large overvoltage for H_2 evolution compared with the other metals [17]. For the other three metals the ranking for coverages less than 10^{-7} mol cm^{-2} is Rh > Pt > Pd. When the coverage of metal is greater than about 10^{-7} mol cm^{-2} the differences between platinum and palladium are smaller, but rhodium remains the superior catalyst for H_2 evolution from the $[(PQ^{+})_n]_{surf}$ polymer.

Figure 7 shows steady state current density–voltage curves for rotating disk indium tin oxide (ITO) electrodes derivatized with I followed by various coverages of rhodium. (The ITO was deposited onto platinum flag electrodes using a Materials Research Corporation model 8620 r.f. sputtering system operating at about 200 W power output. A pressed-powder ITO target was sputtered for about 30 min to give a thickness of ITO sufficient to cover the platinum and to block H_2 evolution from the platinum.) The ITO electrode is representative of electrode surfaces having a large overvoltage for H_2 evolution. As shown in Fig. 7, negligible steady state current for H_2 evolution occurs for either naked ITO or ITO/$[(PQ^{2+/+})_n]_{surf}$ for electrode potentials near $E^{\circ\prime}(H_2O/H_2)$. Clearly, the deposition of rhodium onto the $[(PQ^{2+/+})_n]_{surf}$ or directly onto the ITO gives significant catalysis of H_2 evolution. A naked platinum disk gives an H_2 evolution rate that is directly proportional to $\omega^{1/2}$ at −0.78 V (SCE) and which is included in Fig. 7(a) for comparison. The lack of a current plateau indicates that i_E does not completely limit the H_2 evolution for the rhodium coverages shown. Also, since the i_L limit is much higher (*cf.* the naked platinum curve), the value of i_k is the limiting factor. The strong dependence on potential is consistent with an i_k limitation. It is noteworthy that i_{obs} exceeds 25 mA cm^{-2} for the rhodium coverage of 6.6×10^{-8} mol cm^{-2}, a significantly better performance than that achieved with palladium [9].

A significant finding is that the values of i_{obs} far exceed i_E when the coverages of the most active metals exceed 10^{-7} mol cm^{-2} (Figs. 6 and 7). At first this seems like an inexplicable result, since the redox conduction of the polymer is the only mechanism for equilibration of the electrode with the noble metal. However, as the coverage of metal increases, it is probable that the metal is not restricted only to the outermost surface of the polymer. Instead, the noble metal is likely to be penetrating the polymer, significantly reducing the separation of the electrode from the catalyst particles. Under such circumstances the value of i_E determined by measuring i_{obs} for the mediated reduction of $Ru(NH_3)_6^{3+}$ at the outermost surface of the polymer is an inappropriate limit for the generation of H_2. Auger depth profile analyses qualitatively show that the larger coverages of metal do extend further into the polymer.

The electrochemical results for H_2 evolution at high coverages of the catalytic metal are consistent with the fact that the metal penetrates into

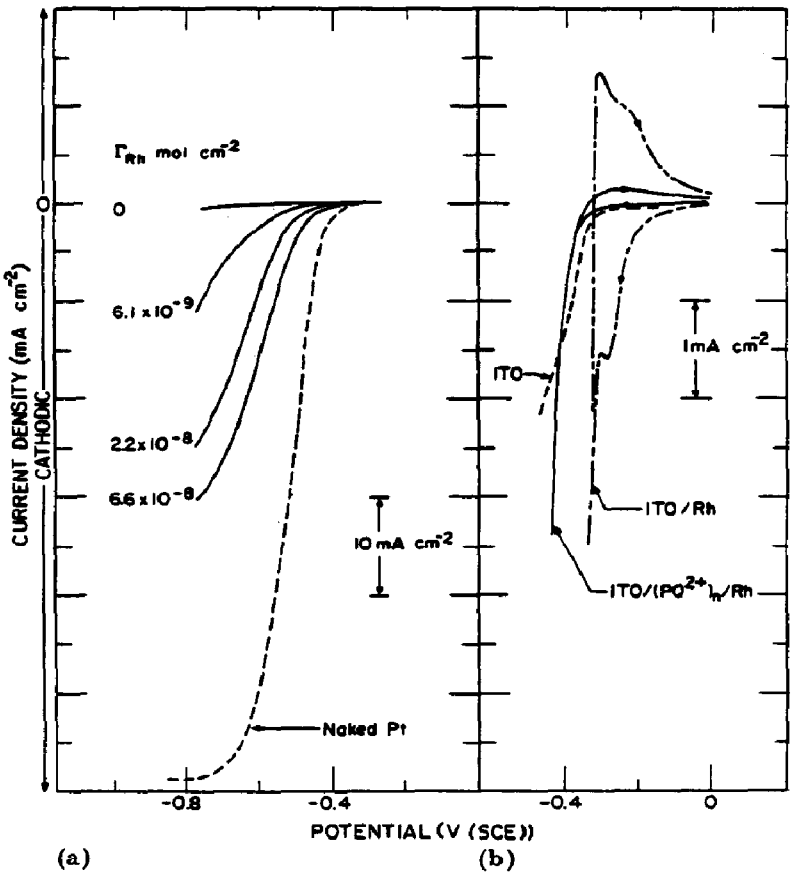

Fig. 7. (a) Current density–voltage curves for an ITO/$[(PQ^{2+})_n]$/Rh_{surf} electrode (———) with increasing Γ_M ($\omega^{1/2}$ = 12; solution, 0.2 M $ClCH_2COOH$ and 1 M KCl; pH 2.8). The coverage of $[(PQ^{2+/+})_n]_{surf}$ is about 4×10^{-8} mol cm^{-2} and gives a negligible current for the $[(PQ^{2+})_n]_{surf} \rightleftarrows [(PQ^{+})_n]_{surf}$ interconversion at the current scale shown (sweep rate, 10 mV s^{-1}). The current at a naked platinum disk of the same area (— — —) is shown for comparison. (b) Comparison of ITO, ITO onto which rhodium was deposited, and the ITO/$[(PQ^{2+/+})_n]$/Rh_{surf} in 0.5 M H_2SO_4 (sweep rate, 100 mV s^{-1}). (It should be noted that the ITO/$[(PQ^{2+})_n]$/Rh_{surf} electrode ($\Gamma_{Rh} = 6.6 \times 10^{-8}$ mol cm^{-2}) gives an onset at the potential for reducing $[(PQ^{2+})_n]_{surf}$ and not at $E^{\circ\prime}(H^+/H_2)$, indicating that the rhodium is not in direct contact with the ITO surface.)

the polymer, but the Auger depth profile analysis shows that the metal does not directly contact the electrode surface. Electrochemical results are in accord with the conclusion that the redox conduction of the polymer remains the only mechanism for equilibration of the electrode with the noble metal catalyst. Figure 7(b) shows the current density–voltage curves in 0.5 M H_2SO_4 for ITO, ITO/Rh and the ITO/$[(PQ^{2+})_n]$/Rh_{surf} electrode used in Fig. 7(a). The current response at the ITO/$[(PQ^{2+})_n]$/Rh_{surf} electrode with $\Gamma_{Rh} = 6.6 \times 10^{-8}$ mol cm^{-2} closely tracks that of naked ITO. When rhodium contacts the ITO substrate, current is observed at more positive

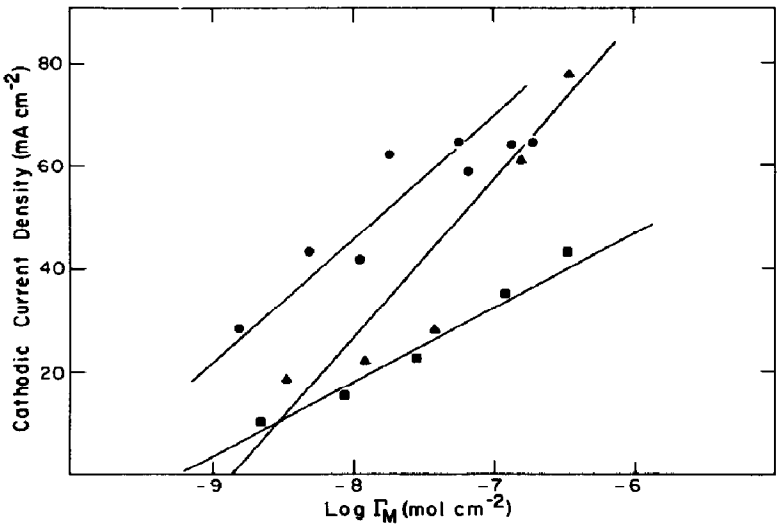

Fig. 8. Plot of current density for H_2 evolution at ITO/M rotating disk electrodes for M ≡ Pd, Pt, Rh as a function of coverage of M ($\omega^{1/2}$ = 16; electrode potential, −0.78 V (SCE); solution, 0.2 M $ClCH_2COOH$ and 1 M KCl; pH 2.8): ●, rhodium; ▲, platinum; ■, palladium. (The metals were plated as described in the caption for Fig. 6; the electrodes are characterized by data as for the polymer-modified electrodes in Fig. 6.)

potentials, and in the current density–voltage curves waves for the formation and reoxidation of a rhodium hydride are seen. Even at the highest metal coverages studied the $[(PQ^{2+})_n]_{surf}$ film can separate the noble metal from the electrode substrate.

The activity of metal deposited directly onto ITO substrates was also investigated, to provide a comparison for the results obtained on polymer-modified surfaces. Figure 8 shows the current density for H_2 evolution as a function of noble metal and coverage in a solution of 0.2 M $ClCH_2COOH$ and 1 M KCl of pH 2.8 at rotating ($\omega^{1/2}$ = 16) metal-modified ITO electrodes held at −0.78 V (SCE). For these electrodes the current was rotation dependent, so i_{obs} does not represent the maximum current possible. For rhodium and platinum the highest coverages yield electrodes that give linear Levich plots; however, palladium was much less active than this. For low coverage the ordering of catalyst activity is again Rh > Pt > Pd, as found for the metals deposited onto the redox polymer. Current densities close to the maximum values attained for platinum and palladium on ITO/$[(PQ^{2+})_n]$/M_{surf} electrodes at −0.78 V (SCE) are obtained at ITO/M electrodes at the same potential with approximately 100 times less metal. Films of $[(PQ^{2+})_n]$/Rh_{surf} are relatively more active, requiring about ten times more rhodium to give the same current at rhodium deposited on ITO. However, the activity at polymer-modified surfaces is related in part to the rate of charge transport from the electrode, through the polymer, to catalyst sites. Since this factor cannot be evaluated at high metal coverages where i_E is not known, a direct comparison of metal activity i_k for the two types of modified ITO surface is difficult. Nonetheless, it is apparent that at low metal coverage on the

polymer where the value of i_E is approximately equal to that found from the mediated reduction of $Ru(NH_3)_6^{3+}$ the metal on the polymer is less active than when it is deposited directly onto ITO. For palladium the polymer appears to lower activity by at least a factor of 10 under such conditions [9, 10].

The results for the generation of H_2 from the $[(PQ^{2+/+})_n]/M_{surf}$ systems allow several conclusions. First, significant current densities (more than 25 mA cm^{-2}) for H_2 generation can be obtained for sufficient coverages of the metal. Second, rhodium is the superior material of the group silver, rhodium, palladium and platinum, giving the highest catalytic activity and giving i_{obs} in excess of 25 mA cm^{-2} with the lowest coverage. Third, there appears to be evidence at the higher metal coverages that the polymer can serve as a three-dimensional zone of catalytic activity to improve i_{obs}; the fact that i_{obs} can significantly exceed i_E is the principal evidence that H_2 evolution is not constrained to the outermost surface of the catalyst. Finally, though the polymer can be a zone of three-dimensional activity, the catalytic activity of the metal is less than that on ITO surfaces. The inability to know the proper value of i_E for the case where the metal penetrates the polymer precludes quantitative evaluation of i_k, so conclusions regarding the activity of the metal catalyst at high coverages of metal are qualitative.

2.3. Surface modification of p-InP photocathodes

The discovery that deposited rhodium is the superior catalytic metal when deposited onto redox polymers has stimulated us to assess the behavior of photocathode/redox polymer/rhodium assemblies for the photogeneration of H_2. Additionally, the properties of the polymer derived from the cobalticenium reagent II are superior to those of polymers derived from I in that the cobalticenium is more transparent and is more durable in aqueous solutions at very negative potentials [8]. The improved durability probably derives from the fact that $[(CoL_2^{+/0})_n]_{surf}$ has only one redox system whereas for $[(PQ^{2+/+})_n]_{surf}$ further reduction to $[(PQ^0)_n]_{surf}$, which is not durable in aqueous media, is easily accessible. The value of $E^{\circ\prime}[(CoL_2^{+/0})_n]_{surf}$ is about −0.6 V (SCE) [8], and the charge transport properties are similar to those of $[(PQ^{2+/+})_n]_{surf}$. The results for p-Si/$[(CoL_2^{+/0})_n]$/Rh_{surf} show similar performance for photoelectrochemical H_2 evolution to p-Si/$[(PQ^{2+/+})_n]$/Pd_{surf} [8], but optimization of the systems has not yet been undertaken. Figure 3 shows the Auger depth profile analysis for a p-Si cathode studied in this regard [8].

Derivatization of p-InP should lead to higher efficiencies for H_2 evolution than is possible with p-Si, and some preliminary results with p-InP/$[(PQ^{2+/+})_n]_{surf}$/Pd are quite promising [22]. However, unlike p-Si, the surface chemistry of ⟨111⟩B-oriented p-InP is not as conducive to functionalization with silane reagents like I and II because there is not a stable oxide. Recently, it has been discovered [10] that $BrCH_2CH_2OH$ will react with a ⟨111⟩B-oriented p-InP surface pretreated with Br_2–MeOH in such a way as to promote the binding of the silane reagent II. The rationale for the use of

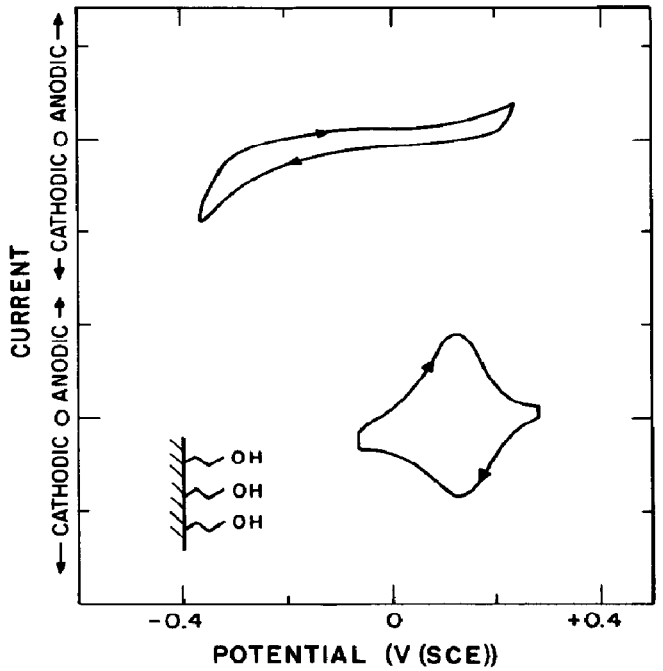

Fig. 9. Cyclic voltammetry of ⟨111⟩B-oriented p-InP under 632.8 nm illumination (about 40 mW cm^{-2}) after derivatization with reagent II for different InP pretreatments [11]: (a) a 20 min exposure to CH_3CH_2OH at about 333 K after a Br_2–MeOH etch; (b) a 20 min exposure to $BrCH_2CH_2OH$ (1 vol.% in CH_3CN) at about 60° after a Br_2–MeOH etch.

$BrCH_2CH_2OH$ was the possibility of reaction of the phosphorus-rich surface with the $BrCH_2CH_2OH$ to give a pendant alcohol group that could react with silane reagents. Whether this rationale corresponds to reality remains to be established, but the derivatization of ⟨111⟩B-oriented p-InP can be carried out successfully using a $BrCH_2CH_2OH$ pretreatment and does not work when using CH_3CH_2OH as a control pretreatment (Fig. 9). Conventional oxide-bearing electrodes, such as degenerate SnO_2 (or silicon, Fig. 3), can be functionalized with reagent II and when compared with the illuminated p-InP give a measure of the photovoltage (Fig. 10). As illustrated by the data in Fig. 10, the reduction of $[(CoL_2^{+})_n]_{surf}$ to $[(CoL_2^{0})_n]_{surf}$ can be effected at a voltage approximately 750 mV more positive on the illuminated p-InP surface than on the conventional electrode surface. Approximately 750 mV is the expected photovoltage for a good p-InP photocathode in aqueous solution [23].

Neither p-InP nor p-InP/$[(CoL_2^{+/0})_n]_{surf}$ is effective in the photoelectrochemical generation of H_2. However, as for the $[(PQ^{2+/+})_n]_{surf}$ system described above, the deposition of noble metals onto the $[(CoL_2^{+/0})_n]_{surf}$ does lead to catalytic H_2 generation [8, 11]. Figure 11 shows photocurrent–voltage curves for small-area p-InP/$[(CoL_2^{+/0})_n]$/Rh_{surf} photocathodes. The pH used is the approximate optimum, giving the highest product of photovoltage, with respect to $E^{o\prime}(H_2O/H_2)$, and photocurrent for H_2 evolution.

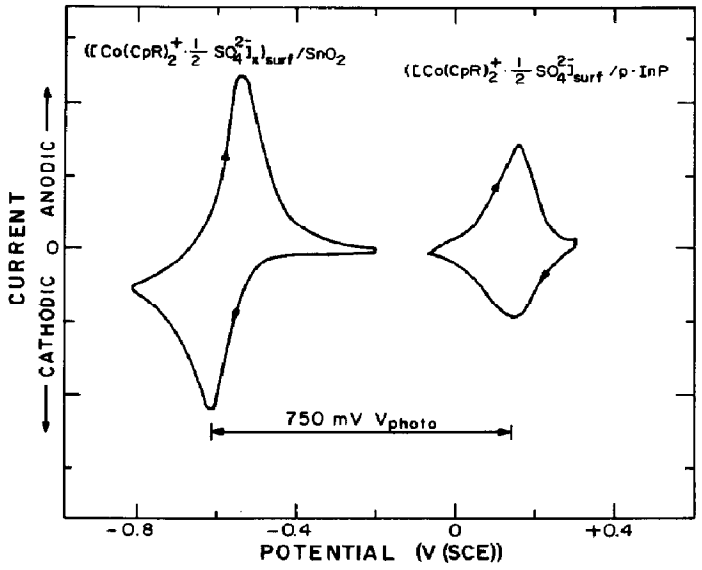

Fig. 10. Comparison of cyclic voltammetry for SnO_2 and illuminated p-InP in aqueous 1.0 M Na_2SO_4 after derivatization with reagent II, showing approximately 750 mV photovoltage for the p-InP (sweep rate, 20 mV s^{-1}).

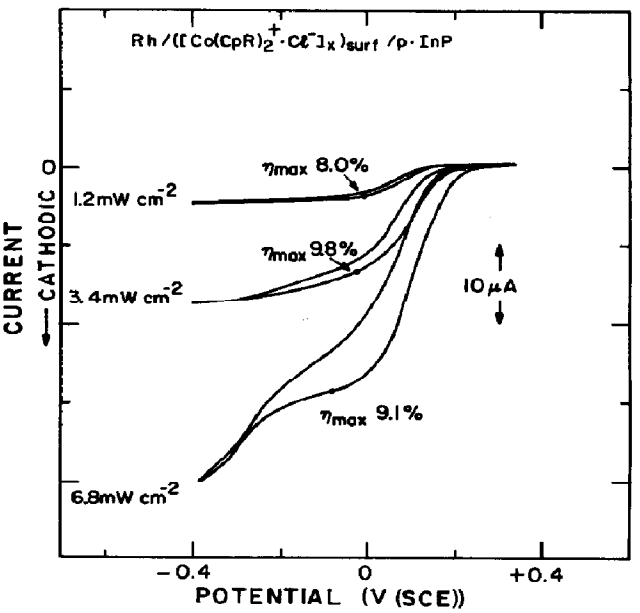

Fig. 11. Photocurrent–voltage curves for H_2 generation from p-InP/[$(CoL_2^{+/0})_n$]$_{surf}$/Rh photocathodes under 632.8 nm illumination (pH 3.8; $E^{o\prime}$ = —0.47 V (SCE); $\Gamma_{polymer}$ = 1.2×10^{-7} mol cm^{-2}; $\Gamma_{Rh} = 4.0 \times 10^{-8}$ mol cm^{-2}; sweep rate, 2 mV s^{-1}).

Low light intensity at 632.8 nm gives an efficiency of the order of 10%. The efficiency at solar intensities declines, presumably because both i_E and i_k limit the photocurrent for the device shown. For the system shown the

coverage of 1.2×10^{-7} mol cm^{-2} of $[(CoL_2^{+/0})_n]_{surf}$ restricts i_E significantly [8]. Even for low light intensities the efficiency falls far short of the best efficiencies for p-InP-based H_2 generation cells [1]. Additional effort to develop redox polymer/catalyst assemblies having very large i_k and i_E values is required in order to realize practical efficiencies. Exploitation of the three-dimensional zone of catalyst activity as a means of improving efficiency is viable, but the generation of a gaseous product at high current density (25 mA cm^{-2}) would lead to mechanical destruction of the polymer/catalyst assembly by the gas bubbles. However, as illustrated below, for the generation of solution reduction products the three-dimensional zone of reactivity can be quite useful.

2.4. Electrochemical and photoelectrochemical reduction of aqueous CO_3H^-

While several metals are known to be relatively effective catalysts for the evolution of H_2 from H_2O, *e.g.* rhodium, platinum and palladium, the development of catalysts for the reduction of aqueous CO_2 has been modest. Intense interest exists in effecting the light-driven reduction of CO_2. Solar generation of liquid and gaseous alcohol or hydrocarbon fuels that could be burned in air is a long-term objective that requires the development of new catalysts for the reduction of aqueous CO_2. Recent work in our laboratory has demonstrated that high surface area palladium will effect the equilibrium represented by the following equation at 298 K and 1 atm H_2 [24]:

$$H_2 + CO_3H^-(aq) \overset{\text{"Pd"}}{\rightleftharpoons} HCO_2^-(aq) + H_2O \quad (6)$$

Heretofore only biological enzymes were known to be effective in this system under such mild conditions [25]. The generation of HCO_2^- under mild conditions indicates that the reduction of aqueous CO_2 (CO_3H^-) can be effected electrochemically and photoelectrochemically without significant overvoltage. Indeed, since H_2 can be generated photoelectrochemically with more than 10% efficiency [1], it can be concluded that HCO_2^- could be generated with similar efficiency by using the H_2 to reduce the CO_3H^-. The lack of a loss in efficiency stems from the fact that the equilibrium constant is approximately unity for the system represented by eqn. (6) [24].

The finding that the equilibrium constant for eqn. (6) is about unity means that $E^{\circ\prime}(H_2O/H_2) \approx E^{\circ\prime}(CO_3H^-/HCO_2^-)$ in aqueous solution containing CO_3H^- and HCO_2^-. Accordingly, the reduction of CO_3H^- to HCO_2^- can, in principle, be effected electrochemically using high surface area palladium-based catalysts in equilibrium with an electrode. The system represented by Fig. 12 has been investigated for the electrochemical [12] and photoelectrochemical reduction of aqueous CO_3H^-. In the catalyst system the redox polymer provides a mechanism for the direct equilibration of the electrode with the dispersed palladium catalyst for the reduction represented by the following equation:

$$CO_3H^- + H_2O + 2e^- \longrightarrow HCO_2^- + 2OH^- \quad (7)$$

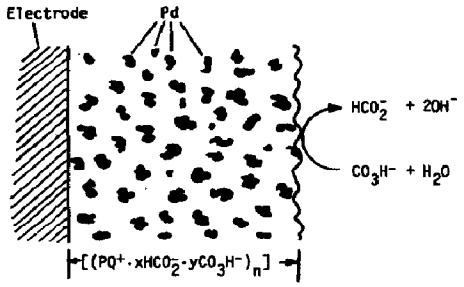

Fig. 12. Catalytic system for the electrochemical reduction of aqueous CO_3H^- to HCO_2^-.

TABLE 1

Electrochemical and photoelectrochemical reduction of aqueous CO_3H^- to HCO_2^- [a]

Cathode	*Starting solution*[b]	*Ultimate concentration of* HCO_2^-[c] (mol l^{-1})	*Current efficiency* (%)
$W/[(PQ^{2+} \cdot Pd)_n]_{surf}$[a]	1.0 M $Na[CO_3H]$	0.09	80
$Pt/[(PQ^{2+} \cdot Pd)_n]_{surf}$[d]	1.0 M $Na[CO_3H]$	0.11	75
$Pt/[(PQ^{2+} \cdot Pd)_n]_{surf}$[d]	3.0 M $Cs[CO_3H]$	0.18	80
$Pt/[(PQ^{2+} \cdot Pd)_n]_{surf}$[d]	3.0 M $Cs[CO_3H]$	0.32	81
$Pt/[(PQ^{2+} \cdot Pd)_n]_{surf}$[d]	6.0 M $Cs[CO_3H]$	0.38	73
$Pt/[(PQ^{2+} \cdot Pd)_n]_{surf}$[d]	6.0 M $Cs[CO_3H]$	0.53	74
$p\text{-}Si/[(PQ^{2+} \cdot Pd)_n]_{surf}$[e]	3.0 M $Cs[CO_3H]$	0.02	70
$p\text{-}Si/[(PQ^{2+} \cdot Pd)_n]_{surf}$[e]	3.0 M $Cs[CO_3H]$	0.02	75

[a] Controlled potential electrolysis mode where the cathode (17 cm^2) potential was slowly moved toward more negative values to maintain approximately 0.5 mA current. The final cathode potential was no more negative than −0.80 V (SCE).

[b] A specially designed small-volume E-shaped three-compartment Pyrex cell was used. The working cathode compartment and the counterelectrode compartment containing 2 - 5 ml CO_3H^- solution at the ends were separated by the fine glass frits of the middle compartment also filled with CO_3H^- solution. The counterelectrode compartment contained a silver gauze anode to suppress O_2 evolution and the middle compartment contained an SCE as reference. The glass tubing bodies of the electrodes were sealed to the cell using O-ring thermometer adaptors to prevent equilibration with air.

[c] Monitored by ^1H or ^{13}C nuclear magnetic resonance or by enzyme assay. The error limit is ±10% [12].

[d] Controlled current electrolysis mode where the cell current was maintained at 0.5 - 0.8 mA throughout the entire experiment depending on the size of the cathode (about 15 - 25 cm^2). The potential of the working cathode was monitored and did not exceed −0.80 V (SCE) at the end of the electrolyses.

[e] Measured under visible light illumination at approximately 100 mW cm^{-2} from a tungsten filament lamp. The p-Si photocathode (about 2 cm^2) potential was slowly moved from an initial value of 0 V (SCE) to a more negative value to give a photocurrent of approximately 0.5 mA. This cell current was maintained until the photocathode was poised at −0.60 V (SCE) when the electrolyses were terminated. The photovoltage with respect to $E^{\circ\prime}(CO_3H^-/HCO_2^-)$ was greater than or equal to 150 mV throughout the photoelectrolysis.

Conventional electrode materials such as tungsten or platinum derivatized with I followed by impregnation with palladium give the reduction of CO_3H^- to HCO_2^- with more than 70% current efficiency within 50 mV of $E^{\circ\prime}(CO_3H^-/HCO_2^-)$. Table 1 gives some representative results.

Photoelectrochemical reduction of CO_3H^- at illuminated p-Si/$[(PQ^{2+/+}\cdot Pd)_n]_{surf}$ electrodes has also been carried out, and some results are included in Table 1. For the conventional electrochemical reduction the generation of greater than 0.5 M HCO_2^- has been demonstrated, but the photoelectrochemical production has yielded lower absolute amounts of HCO_2^-. However, the current efficiencies in both instances can be high. The optical-to-chemical conversion efficiency is no greater than about 1% with the p-Si/$[(PQ^{2+/+}\cdot Pd)_n]_{surf}$ system because i_k and i_E are low, and the catalyst assembly absorbs a significant fraction of the incident visible light. Nonetheless, the reduction of CO_3H^- to HCO_2^- can be effected in an uphill sense at the catalytic photocathode. The results represent a modest beginning toward light-driven generation of reduced products from CO_2 and H_2O.

3. Conclusions

Effective electrode-bound catalysts for H_2 evolution can be derived from combinations of a redox polymer and a noble metal. Of the metals investigated (silver, palladium, platinum and rhodium) rhodium is the superior catalyst. Only one of these metals is effective in the electrochemical reduction of CO_3H^- to HCO_2^-, namely palladium. The $[(PQ^{2+}\cdot Pd)_n]_{surf}$ catalyst system can produce greater than 0.5 M HCO_2^- at electrode potentials near $E^{\circ\prime}(CO_3H^-/HCO_2^-)$, but the catalytic activity of the $[(PQ^{2+/+}\cdot Pd)_n]_{surf}$ system is too low to give highly efficient solar-driven production of HCO_2^-. The new cobalticenium-based derivatizing reagent II can be used to functionalize appropriately pretreated p-InP. The deposition of rhodium onto the surface catalyzes the generation of H_2, and monochromatic 632.8 nm illumination at low light intensity gives an overall energy conversion efficiency of about 10%. Additional effort is needed to develop new photoelectrode catalyst systems for solar-driven fuel formation if direct fuel formation is to approach the high efficiencies now possible for photoelectrochemical electricity generation.

Acknowledgments

We are grateful for support from the U.S. Department of Energy, Office of Basic Energy Sciences, Division of Chemical Sciences. D.J.H. acknowledges partial support as a National Science and Engineering Research Council Predoctoral Fellow (1980 - 1984). The use of the Central Facilities of the Massachusetts Institute of Technology Center for Materials Science and Engineering is appreciated.

References

1 A. Heller, *Science, 223* (1984) 1141.
2 H. D. Abruña and A. J. Bard, *J. Am. Chem. Soc., 103* (1981) 6898.
3 Y. Nakato, S. Tonomura and H. Tsubomura, *Ber. Bunsenges. Phys. Chem., 80* (1976) 1289.
W. Kautek, J. Gobrecht and H. Gerischer, *Ber. Bunsenges. Phys. Chem., 84* (1980) 1034.
J. A. Baglio, G. S. Calabrese, D. J. Harrison, E. Kamieniecki, A. J. Ricco, M. S. Wrighton and G. D. Zoski, *J. Am. Chem. Soc., 105* (1983) 2246.
4 J. A. Bruce, T. Murahashi and M. S. Wrighton, *J. Phys. Chem., 86* (1982) 1552.
5 D. C. Bookbinder, J. A. Bruce, R. N. Dominey, N. S. Lewis and M. S. Wrighton, *Proc. Natl. Acad. Sci. U.S.A., 77* (1980) 6280.
R. N. Dominey, N. S. Lewis, J. A. Bruce, D. C. Bookbinder and M. S. Wrighton, *J. Am. Chem. Soc., 104* (1982) 467.
D. J. Harrison, G. S. Calabrese, A. J. Ricco, J. Dresner and M. S. Wrighton, *J. Am. Chem. Soc., 105* (1983) 4212.
6 G. S. Calabrese and M. S. Wrighton, *J. Am. Chem. Soc., 103* (1981) 6273.
7 R. A. Simon, A. J. Ricco, D. J. Harrison and M. S. Wrighton, *J. Phys. Chem., 87* (1983) 4446.
8 R. A. Simon, T. E. Mallouk, K. A. Daube and M. S. Wrighton, submitted for publication.
R. A. Simon, *Ph.D. Thesis*, Massachusetts Institute of Technology, 1984.
9 D. J. Harrison and M. S. Wrighton, *J. Phys. Chem., 88* (1984) 3932.
10 D. J. Harrison, *Ph.D. Thesis*, Massachusetts Institute of Technology, 1984.
11 K. A. Daube, T. E. Mallouk and M. S. Wrighton, unpublished.
12 C. J. Stalder, S. Chao and M. S. Wrighton, *J. Am. Chem. Soc., 106* (1984) 3673.
13 A. J. Ricco, *Ph.D. Thesis*, Massachusetts Institute of Technology, 1984.
14 D. E. Bradley, in K. Desmond (ed.), *Techniques of Electron Microscopy*, Blackwell, Oxford, 1967.
15 C. P. Andrieux, J. M. Dumas-Bouchiat and J. M. Saveant, *J. Electroanal. Chem., 131* (1982) 1.
C. P. Andrieux and J. M. Saveant, *J. Electroanal. Chem., 134* (1982) 163.
F. C. Anson, J. M. Saveant and K. Shigahara, *J. Phys. Chem., 87* (1983) 214.
16 A. J. Bard and L. R. Faulkner, in *Electrochemical Methods*, Wiley, New York, 1980.
17 J. O'M. Bockris and A. K. N. Reddy, in *Modern Electrochemistry*, Vol. 2, Plenum, New York, 1970, p. 1238.
18 R. N. Dominey, T. J. Lewis and M. S. Wrighton, *J. Phys. Chem., 87* (1983) 5345.
19 T. J. Lewis, H. S. White and M. S. Wrighton, *J. Am. Chem. Soc., 106* (1984) 6947.
20 D. C. Bookbinder and M. S. Wrighton, *J. Electrochem. Soc., 130* (1983) 1080.
21 M. M. Rosen and A. I. Krasna, *Photochem. Photobiol., 31* (1980) 259.
22 R. N. Dominey, *Ph.D. Thesis*, Massachusetts Institute of Technology, 1982.
23 R. N. Dominey, N. S. Lewis and M. S. Wrighton, *J. Am. Chem. Soc., 103* (1981) 1261.
24 C. J. Stalder, S. Chao, D. P. Summers and M. S. Wrighton, *J. Am. Chem. Soc., 105* (1983) 6318; *106* (1984) 2723.
25 A. M. Klibanov, B. N. Alberti and S. E. Zale, *Biotechnol. Bioeng., 24* (1982) 25.